

DMA and ATR FT-IR Studies of Gas Plasma Modified Silicone Elastomer Surfaces

MAREK W. URBAN* and MARK T. STEWART, *Department of Polymers and Coatings, North Dakota State University, Fargo, North Dakota 58105*

Synopsis

The results obtained from ATR FT-IR and DMA studies of gas/plasma surface modified silicone elastomers are presented. The structural analysis indicates that, upon the plasma treatment in the presence of argon and carbon dioxide gases, the primary components of the surface are short chain layers with carbonyl groups. Their presence significantly influences the viscoelastic properties of the elastomer. The measurements of the storage modulus (E') indicate a substantial decrease of the crosslink density upon the plasma treatment. Although the glass transition temperature also changes, these changes do not follow the trend observed of E' values, and primarily depend on the chemical structures that develop upon the treatment. On the other hand, the ammonia-plasma surface modification introduces surface amide groups on the surface of the silicone elastomer, which effectively contribute to the increase of both T_g and storage modulus of the elastomer.

INTRODUCTION

In recent years silicone elastomers have spun major interest mainly in theoretical studies.¹⁻⁴ While useful theories have provided further understanding of the network formation and predicted various properties of silicone rubbers, only a few experimental approaches have been taken to correlate the macroscopic measurements with the chemistry of crosslinking reactions occurring during the network formation. Recently, we have utilized photoacoustic Fourier transform infrared (PA FT-IR) spectroscopy to *in situ* monitor the crosslinking process of hydroxyl-terminated poly(dimethyl siloxane) (PDMS).^{5,6} In this work, we have demonstrated that, although transmission FT-IR does not provide sufficient sensitivity, it is possible to follow the crosslinking process spectroscopically by using photoacoustic FT-IR detection.

While the network formation is responsible for the bulk properties, in many applications the elastomer surfaces need to be modified in order to achieve desirable surface energy, permeability, or surface functionality. Among various surface modifications, plasma treatments performed in the presence of inert or chemically active gases have been commonly employed. Although such treatments alter the surface properties, the detailed structural characterization of the surface species is needed since it allows one to gain further insights into the surface chemistry of modified elastomers. This is particularly important in light of previous studies performed in the late '60s and early '70s,⁷ which commonly were based on the assumption that the surface crosslink

*To whom correspondence should be sent.

density increases following gas plasma treatments. Later attempts resulted in similar assessments, tentatively assuming that the failure of initial studies to detect the presence of surface species must lead to a higher degree of surface crosslinking.⁸ Apparently, such conclusions were primarily based on macroscopic changes observed on the sample surface, such as wettability, contact angle, and mechanical testing, as well as the lack of information on the molecular level.⁹⁻¹¹

The use of silicone rubbers in various fields including biotechnology offers substantial advantages.¹² One would anticipate, for example, taking advantage of the inertness and flexibility of the silicone rubbers and utilizing them in numerous applications. It is, however, desirable to modify the surface, in order to enhance the compatibility with biological systems or to achieve other desired properties. Thus, one approach is to modify the surface in a controllable way, characterize the structures that are being formed upon the treatment and, on that basis, modify the treatments.

Modification of polymer surfaces by exposure to glow discharge has become common in recent years. It is an accepted means of increasing surface energy and creating active sites, presumably without affecting the bulk chemical or physical properties. Unfortunately, little work has been published on the detailed characterization of gas/plasma treated polymer surfaces. For example, indirect evidence of the presence of surface active species was suggested due to ability to graft foreign species on the surface.¹³ Moreover, due to various reasons, the infrared analysis indicated limited success in identifying surface functional groups.^{7,13,14}

In an effort to advance our knowledge and clarify various aspects related to the structure-property relationships of the gas/plasma surface modified silicone elastomers, we have utilized two approaches: First, the plasma-modified surfaces of the silicone network were analyzed by attenuated total reflection (ATR) FT-IR spectroscopy and, second, the viscoelastic properties were examined by dynamic mechanical analysis (DMA). While the spectroscopic measurements provide information about the structures that develop on the surface upon the gas plasma treatment, the dynamic mechanical measurements reveal how such treatments effect the viscoelastic response of the polymer network upon oscillating force as a function of temperature. Thus, both techniques are capable of providing different levels of information; namely, chemical composition of the surface and mechanical properties.

EXPERIMENTAL

Sample Preparation

General Electric industrial grade silicone tubing (37.5% w/w of SiO₂ filler) was formed into approximately 70 cm loops and installed over the motorized pulleys in the plasma chamber. The plasma chamber, shown in Figure 1, was pumped down to approximately 20 mtorr. Upon initiation of a flow of the desired gas, the chamber was allowed to purge for 15 min with the pressure stabilized at 480 mtorr followed by sample rotation. Radio frequency (RF) power was applied to initiate the glow discharge at the selected power setting. All samples were treated for 10 min. The RF power input and type of gas

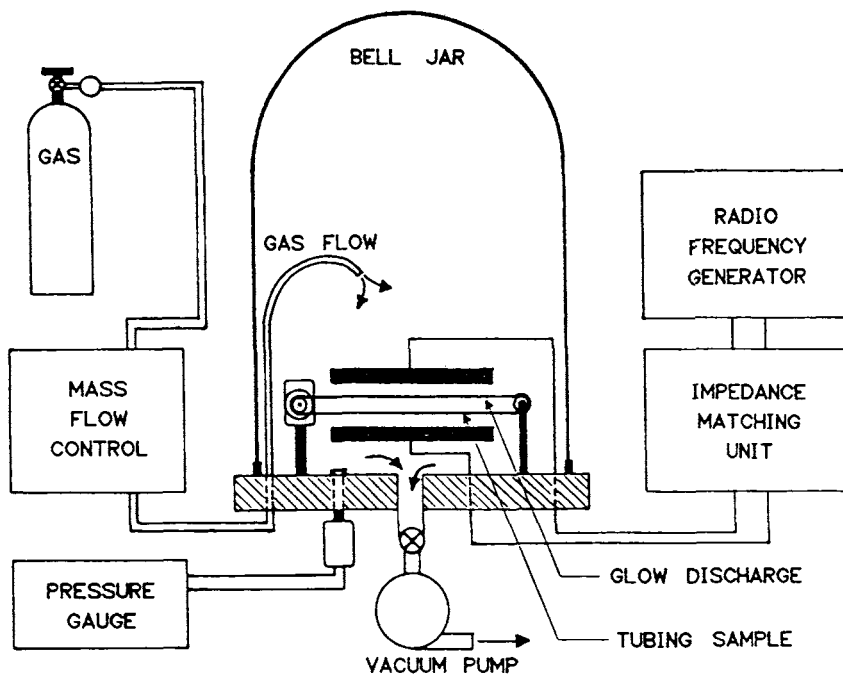


Fig. 1. Plasma treatment chamber and additional equipment.

admitted to the chamber were two variables in the sample treatments. The first set of samples was treated with 2, 10, 50, 100, and 200 W while 50 sccm (stand. cm^3) of argon flowed continuously through the chamber. For the second set, 50 W were applied while argon, carbon dioxide, and ammonia gases were admitted into the sample chamber. All gases (Linde) were ultrapurity grade and were used as supplied.

Plasma treatments were performed in a bell jar vacuum chamber set up with a pair of 20 cm diameter parallel plate electrodes. Power was supplied to the electrodes by an RF Plasma products 13.56 MHz radio frequency generator with an output of 0–500 W. A flow of the gases into the chamber was administered by MKS mass flow controllers. A pair of motorized pulleys allowed continuous rotation of samples through the glow discharge region.

Spectroscopic Measurements

ATR FT-IR spectra were recorded on a Mattson Cygnus-25 single beam spectrometer (Sirius 100) equipped with an He-Ne laser to provide an accuracy in frequency reading of 0.01 cm^{-1} . The ATR attachment (Mattson) with a KRS-5 crystal was aligned to beam incidence angles 30° , 45° , or 60° . The spectrometer mirror velocity was set at 0.316 cm/s . A total of 400 scans were collected in order to achieve a better signal-to-noise ratio. All spectra were ratioed against the reference, KRS-5 crystal. The sample-to-crystal contact was approximately 260 mm^2 . The instrument was purged with purified air supplied from the Balston Filter Products system, type 75-60.

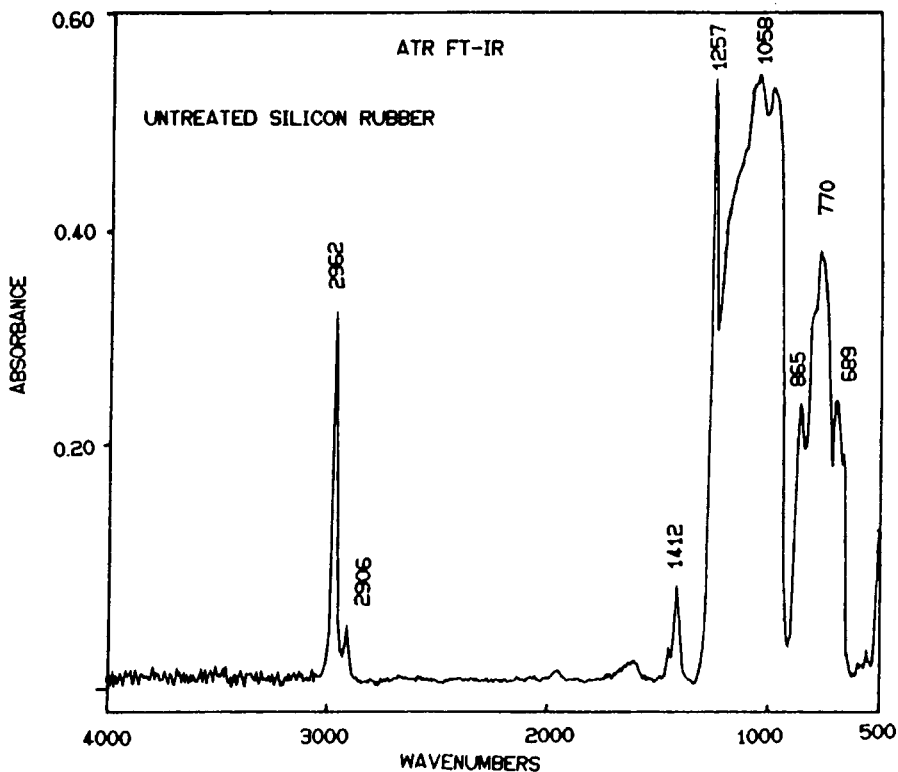


Fig. 2. ATR FT-IR spectrum of untreated silicone rubber surface (angle of incidence 45°).

Dynamic Mechanical Analysis

The DMA measurements were performed in a tensile mode of a DMTA Mk-2 instrument (Polymer Laboratories Inc.) with a frequency of 5 Hz. The silicone tubing (15 mm length) was attached between two clamps, stationary, and movable. The initial parameters were setup as follows: force 0.445 N, strain $\times 4$, and heating rate 5°C min in dry nitrogen atmosphere.

RESULTS AND DISCUSSION

As a starting point of the analysis let us set the stage by defining the infrared active bands observed in the surface ATR spectra of untreated silicone rubber. Figure 2 shows ATR FT-IR spectrum recorded at 45° angle of incidence. This angle provides an approximate penetration depth of about $3.0\ \mu\text{m}$ at $1700\ \text{cm}^{-1}$. As will be seen later on, this spectral range is of a particular interest since various surface modifications lead to the appearance of infrared bands in this region. The same sample spectra, recorded at 30° and 60° , show essentially identical features indicating that no detectable structural differences are found between $1\ \mu\text{m}$ (60°) and $5\ \mu\text{m}$ (30°) at the surface. It is apparent that the untreated surface does not contain products of oxidation which would appear in the $1700\ \text{cm}^{-1}$ region, or other surface impurities. Table I lists the observed bands and their assignments. Although the band assignments have been proposed earlier,^{7,13-15} here they are presented due to

TABLE I
ATR FT-IR Bands in Untreated Silicone Rubber Spectrum
and Their Assignments

| Band (cm^{-1}) | Assignment |
|---------------------------|---|
| 2962 | Asym. C—H stretch |
| 2906 | Sym. C—H stretch |
| 1412 | Asym. CH_3 deform. |
| 1257 | Sym. Si— CH_3 deform. |
| 1058 | Asym. Si—O—R stretch |
| 1020 | Si—O—Si stretch |
| 865 | Si— CH_3 wagging and Si—C sym. stretch. |
| 770 | Si— CH_3 rocking |

various discrepancies reported in the past, and moreover, to formulate the basis for further discussion of the surface analysis of ATR spectra of the silicone rubber surfaces upon the gas/plasma treatments. In the following sections we will discuss how the gas plasma surface treatments influence the surface functionality and the effect of the treatments on viscoelastic properties of the silicone network.

Argon-Plasma Treatments

A commonly employed procedure to modify the silicone surfaces is argon-plasma treatment. As has been proposed in earlier studies, such modification ought to improve the surface properties due to a generation of the higher surface crosslink density.^{8,14,15} Figure 3 shows a series of ATR FT-IR spectra of the Ar/plasma treatments at various plasma power settings. It is noted immediately that upon such treatment, the surface contains carbonyl groups. This is demonstrated by the appearance of a new band at 1725 cm^{-1} with a shoulder at 1720 cm^{-1} . Although inertness of the gas used should prevent the surface from oxidation, it is possible that the residual traces of air present in the sample chamber or trapped in the silica-filled crosslinked network may cause oxidation. In addition, free radicals remaining on the surface after the treatment could react with oxygen when the chamber is vented. Although the source of oxidation is uncertain, it is apparent that the intensity of the carbonyl band reaches a maximum absorbance when the plasma reactor is supplied with 50 W power. This is illustrated in Figure 4, which depicts the intensity of the carbonyl band plotted as a function of supplied power. The treatment at the power settings above 50 W diminishes the amount of oxidative products on the silicone rubber surface. Although such observations may be surprising, since the increased power should lead to a greater extent of oxidation, the energy input provided to the system is so high that ablation removes less stable oxidized surface layers. As a result, the thickness of the newly formed layer is reduced and levels off. Recently, a similar effect of highly energetic ultrasonic waves applied to the surface of PVF_2 was reported.¹⁶ Another possibility, although remote, is that the increased plasma energy results in the formation of species with a higher degree of ionization and such species may be less likely to form carbonyls on the silicone surface. No

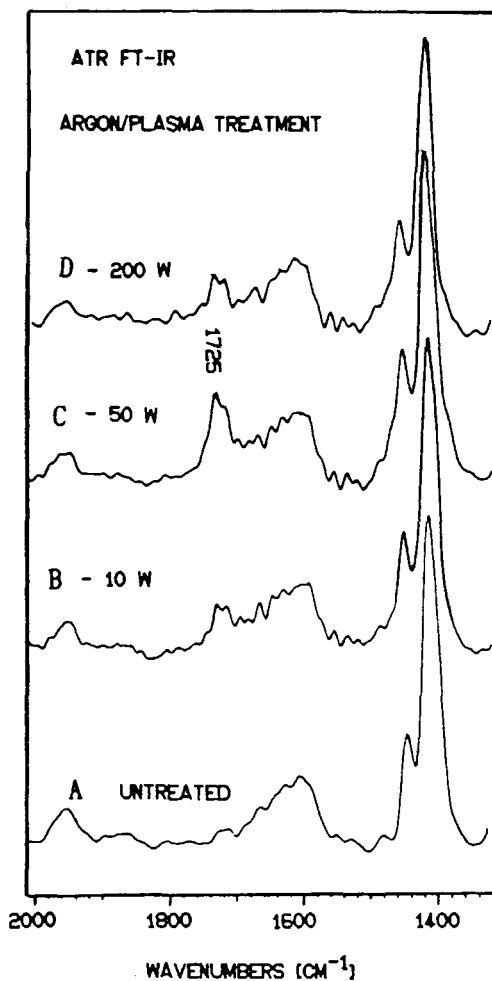


Fig. 3. ATR FT-IR spectra in the 2000–1350 cm^{-1} region of the argon plasma treated surfaces.

spectroscopic evidence for the species containing other than carbonyl groups was found.

As can be gleaned from the literature, there has been an immense amount of information obtained on the polymerization utilizing gas plasma.¹⁷⁻²⁴ However, limited data are available on non-polymer-forming plasma surface treatments.²⁵⁻²⁷ Based on surface studies performed on the silicone elastomers, it has been concluded that the gas plasma modifications increase the degree of crosslinking on the surface.^{8,13} A primary reason for such assessments was attributed to the fact that the silicone surface was somehow modified and in some cases improved, for specific applications. Thus, at this point, is it appropriate to raise the question as to how the surface has been modified? As indicated above, the argon/plasma reaction introduces carbonyl groups on the silicone surface. On the other hand, if upon plasma treatment the surface crosslink density increases (as has been postulated in previous studies), it should be reflected in the changes of glass transition temperatures (T_g) before

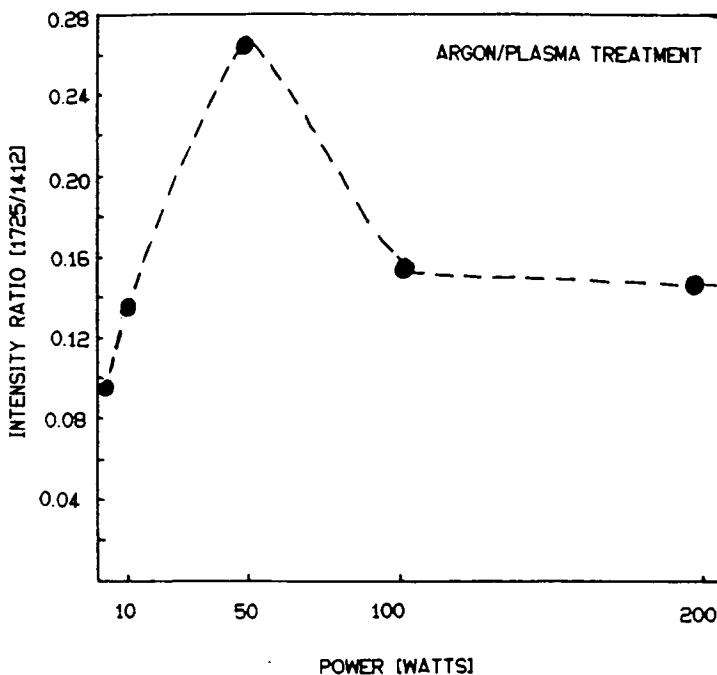


Fig. 4. The intensity ratio of 1725/1412 bands plotted as a function of power.

and after the treatment as well as the changes of the storage modulus ($\log E'$) in a rubbery plateau region (above T_g). For that reason, let us examine the DMA results of Ar/plasma treated silicone elastomer and compare with that of unmodified silicone rubber.

Unlike differential scanning calorimetry (DSC), DMA measurements provide a better accuracy of the glass transition temperature (T_g) readings, and more importantly, are capable of isolating the storage and loss moduli. Postponing temporarily evaluation of the storage modulus above T_g , let us examine how the surface treatment effects T_g . Figure 5(A) illustrates a $\tan \delta$ curve of the untreated silicone specimen. A maximum of the $\tan \delta$ curve appears at -39.0°C , which corresponds to its T_g . It should be noted that the reported T_g value for PDMS is -127°C and the shift to higher temperatures is attributed to the presence of silica filler (37.5% w/w). When the surface is plasma treated in the presence of argon, T_g is shifted to -34.5°C . This is illustrated in Figure 6(A). Such observations could indicate that the raising T_g following surface plasma treatment may indeed reflect larger restrictions of the silicone backbone motions due to an increased degree of crosslinking. Because crosslink density and T_g are important characteristics of the polymer network, the following section will focus on the T_g changes caused by plasma treatment and their relationship to the storage modulus of the system above T_g .

As was demonstrated by Hill and Kozłowski,²⁸ the dynamic measurements are advantageous since it is possible to simultaneously measure storage and loss moduli. Thus, one may determine the storage modulus in a rubbery plateau region (typically, 50°C above T_g) and, by using the theory of rubber

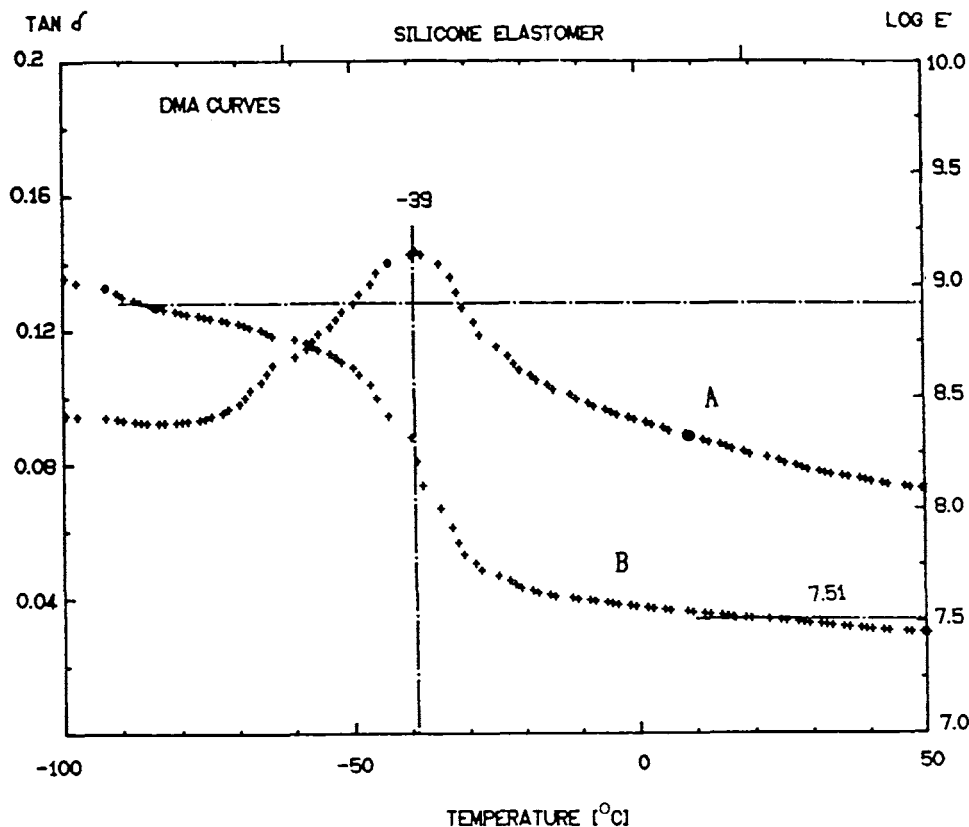


Fig. 5. DMA curves of untreated silicone elastomer: (A) $\tan \delta$; (B) $\log E'$.

elasticity, estimate the network crosslink density. A simplified relationship between crosslink density and storage modulus is given by the following equation²⁹:

$$m_e = E'/3RT$$

where E' is the storage modulus, m_e is the crosslink density, R is the gas constant and T is temperature. The above approach, of course, is simplistic, because the E' measurements do not distinguish between the surface and bulk viscoelastic properties. Moreover, the above equation has been derived from the ideal gas law and hence, we will use it as a "rule of thumb" and compare the storage modulus upon various surface treatments.

Before we begin the analysis of DMA data, let us first recall a general concept commonly employed in the analysis of crosslinked networks. It became almost a custom to correlate T_g with crosslink density of polymer network. For example, upon certain treatment of a given system, the higher T_g should indicate the increase of crosslink density. If such a generalization was correct, the increase of T_g should be accompanied by the increase of E' values in the rubbery plateau region. The first striking observation depicted in Figure 6 is that, upon argon/plasma treatment, T_g increases (trace A) while

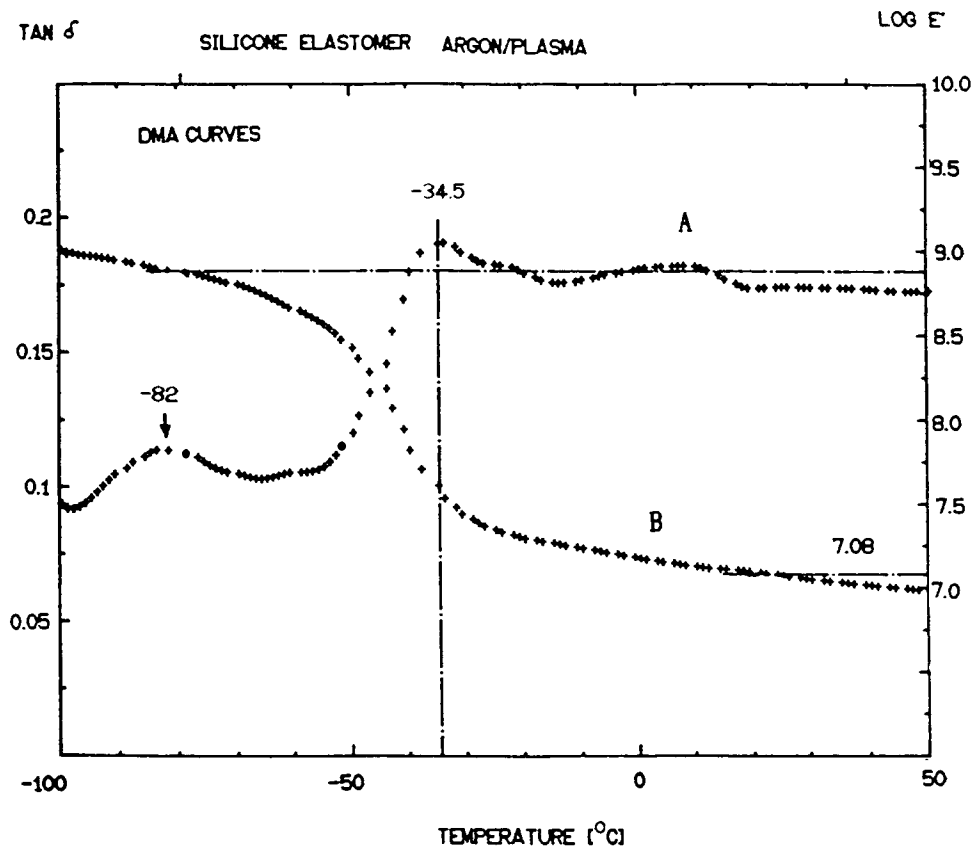


Fig. 6. DMA curves of argon/plasma surface modified elastomer: (A) $\tan \delta$; (B) $\log E'$.

$\log E'$ decreases, from 7.51 for the untreated sample [Fig. 5(B)] to 7.08 for the treated one [Fig. 6(B)]. These results are summarized in Table II along with other surface treatments which will be discussed later on. A comparison of the $\log E'$ values for untreated and argon/plasma treated silicone elastomers indicates that the crosslink density decreases with treatment. On the other hand, the same comparison of the T_g values would suggest that the crosslink density increases. At first glance, the use of T_g as a measure of the crosslink density would lead to an opposite answer. In view of the above considerations, one needs to find the origin of such behavior. Let us go back to the infrared

TABLE II
 $\log E'$ and T_g Values as a Function of Gas/Plasma Treatment^a

| $\log E'$ | T_g [$\tan \delta$ (max)] (°C) | Surface treatment |
|-----------|--------------------------------------|-------------------|
| 7.5 | -39.0 | Untreated |
| 7.08 | -34.5 | Argon (50 W) |
| 7.3 | -42.0 | Carbon dioxide |
| 7.9 | -34.0 | Ammonia |

^a $\log E'$ recorded 50°C above T_g .

analysis and recall that the formation of an oxidative surface layer was detected. Such species have usually higher T_g due to the presence of polar groups and relatively weak elastic response. Although the T_g changes are related to the chemical composition of the oxidative layer, lower $\log E'$ values result from the presence of shorter chains with less motion restrictions. Thus, the presence of such species on the surface will lead to the increase of T_g and lower storage modulus values above T_g .

Although the primary purpose of the DMA measurements was to establish the relationship between glass transition temperature and viscoelastic behavior of the surface modified silicone network, let us focus on $\tan \delta$ curves [Figs. 5(A) and 6(A)]. As shown in Figure 6(A), in addition to a major T_g at -34.5°C , another transition at -82°C is observed. This transition does not appear in the untreated silicone rubber [Fig. 5(A)]. It has been proposed that the low temperature transitions often result from so-called secondary relaxation (loss) processes, and occur due to energy absorption by a polymer at a given frequency of oscillation and temperature. Apparently, shorter segments resulting from the oxidation of the silicone elastomer surface may absorb energy, and, as the plasmons attack the surface, generation of free radicals, ions, and various intermediates lead to the chain scission and subsequent formation of the oxidative products detected in ATR FT-IR spectra. Although in the case of the surface-modified silicone network it is difficult to access precisely the origin of the -82.0°C transition, it probably involves rotations about chemical bonds in the polymer backbone of the surface or near surface species. Such transitions have been proposed for polyethylene due to crankshaft motions of four to six carbons,³⁰ or in poly(ethylene terephthalate)³¹ as a result of methylene or carboxyl group rotations. As a matter of fact, if low temperature transitions are indeed attributed to the rotations of backbone units, shorter segments of the surface with a relatively high degree of freedom can absorb energy at a frequency close to that of the frequency of the motion. The shorter segments of the silicone elastomer surface result from the chain scission followed by oxidation of the surface. Thus, the presence of a low temperature transition is indicative of the surface species with a higher degree of freedom.

Based on the above discussion, it is interesting to note that the viscoelastic behavior ($\log E'$) as well as the glass transition temperature of silicone elastomers are strongly affected by the presence of surface layers. Although the viscoelastic behavior in the rubbery plateau region shows rather unexpected trends, the appearance of a low temperature transition seems to be related to the decrease of E' values above T_g . If the low temperature transition indicates the presence of shorter segments on the elastomer surface, it should certainly be reflected in the viscoelastic response above T_g , since the generation of shorter segments will diminish the crosslink density. On the other hand, the chemistry of the surface will influence the net effect on T_g . In both cases, DMA measurements provide sufficient sensitivity in detecting the effects of surface treatment. The oxidative layers produced during the plasma treatment have thickness no greater than $10\ \mu\text{m}$, whereas a total specimen thickness is about 1 mm. Such comparison demonstrates high sensitivity of DMA measurements. In spite of the fact that this technique provides information about viscoelastic properties as a function of temperature, it is sensitive to the surface treatment.

Carbon Dioxide Plasma Treatment

Figure 7(A) shows ATR FT-IR spectra of the silicone rubber surfaces treated in the presence of carbon dioxide. Similarly to the argon/plasma treatment, the presence of carbon dioxide leads to the formation of carbonyl groups on the silica surface. This is demonstrated by the presence of two carbonyl bands, free C=O stretching mode at 1725 and 1700 cm^{-1} , due to hydrogen-bonded carbonyl groups. However, in contrast to the argon/plasma treatment, two additional bands at 1675 and 1596 cm^{-1} are observed, due to the C=O and C=C stretching vibrations, respectively.³³ With the band assignments given above, the 1725 and 1596 cm^{-1} bands are attributed to the $-\text{O}-\text{CO}-\text{C}(\text{CH}_3)=\text{CH}_2$ species attached to the silicone backbone.³³ Although the band at 1700 cm^{-1} is most likely due to the hydrogen-bonded carbonyls, it may be also attributed to the carbonyl groups in the β position with respect to silicone. Such behavior arises from the inductive effect of the $\text{R}_3\text{SiC}-$ groups associated with the free ends of the polymer backbone.²¹

One of the essential advantages of ATR FT-IR spectroscopy comes from the fact that it is possible to perform surface depth profiling measurements by changing an angle of incidence of incoming light. A comparison of traces A

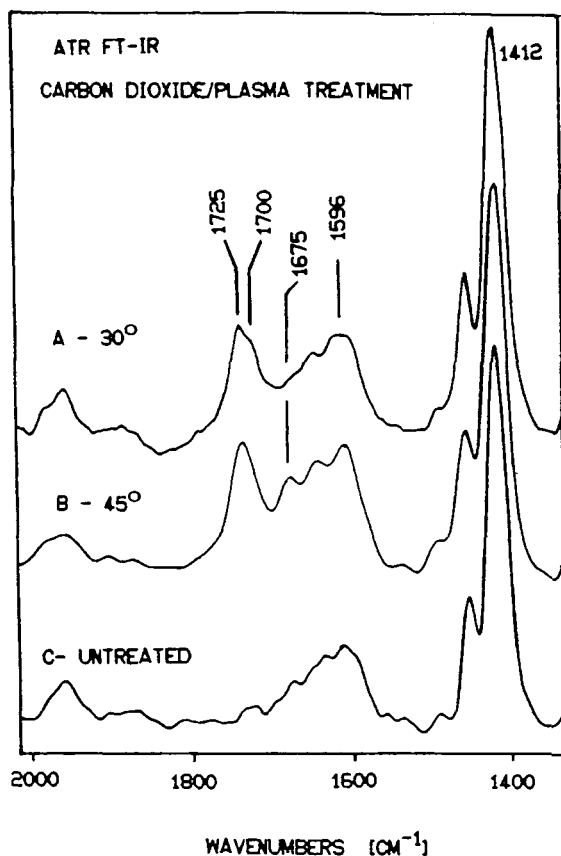


Fig. 7. ATR FT-IR spectra in the region 2000–1350 cm^{-1} of the CO_2 plasma treated surfaces: (A) 30° (angle of incidence); (B) 45°; (C) untreated (45°).

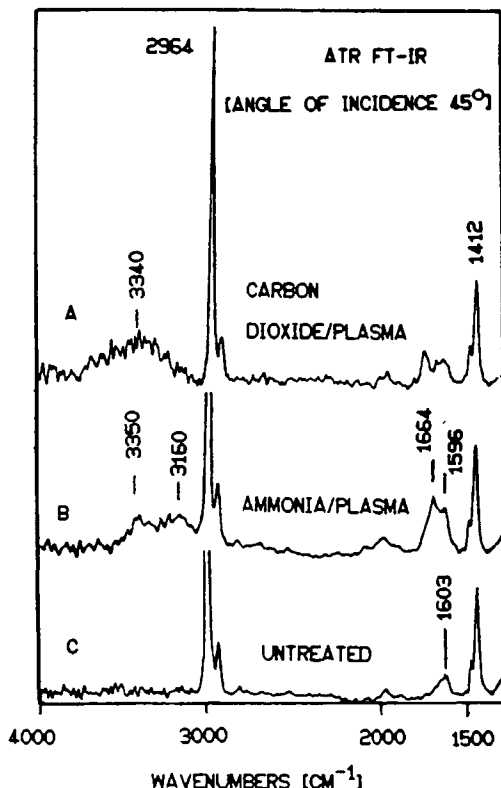


Fig. 8. ATR FT-IR spectra in the region 4000–1300 cm^{-1} .

and B of Figure 7 indicates that the 1700 cm^{-1} band is not present when the incident light strikes at 45° , indicating that a greater extent of hydrogen bonding occurs closer to the surface. In order to further reveal the nature of the surface groups, let us examine the 3700–3200 cm^{-1} region. As illustrated in Figure 8(A) a broad band with a maximum at 3340 cm^{-1} is observed, and indicates formation of the hydrogen bonded $-\text{Si}(\text{OH})$ dimers on the silica surface. The origin of these species arises from the addition of silica filler which acts as a reinforcing agent to the silicone elastomer. Its presence introduces hydroxyl groups, which upon bonding with the hydroxyl terminated silicone network, form the structure such as that shown schematically in Figure 9. The silica particles are built into the polymer network and are held by either hydrogen bonded dimers or $\text{Si}-\text{O}-\text{Si}$ linkages.

In contrast to the argon-plasma treatments, examination of the $\tan \delta$ and $\log E'$ curves, shown in Figure 10, reveals new features. Let us focus on the $\log E'$ and T_g values depicted in Figure 10 and compare them to other gas-plasma treatments listed in Table II. Similarly to the argon plasma, it appears that the $\log E'$ value for carbon dioxide/plasma treatment is lower than that of the untreated specimen. This is accompanied by also lower glass transition temperature, which appears to be -42°C . As we recall, upon Ar-plasma treatment, T_g was higher than that of the untreated sample. The fact that, in both cases, the $\log E'$ values are lower suggests more viscous

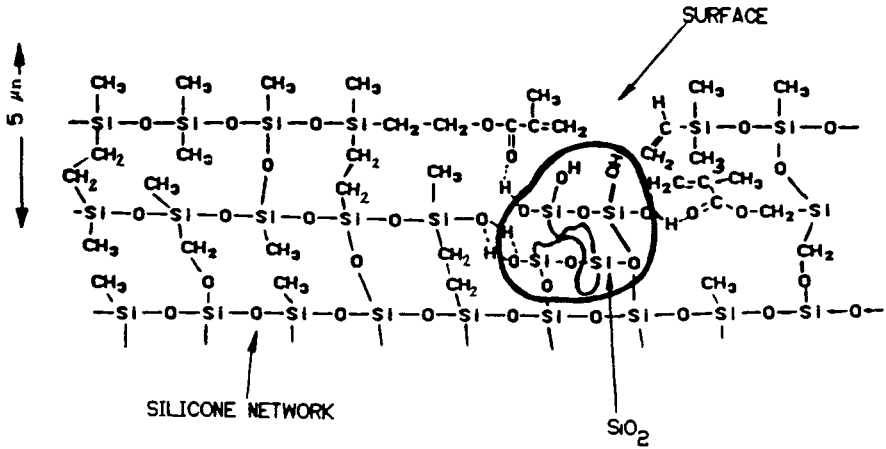


Fig. 9. Proposed model of the CO₂/plasma treated silicone elastomer surface.

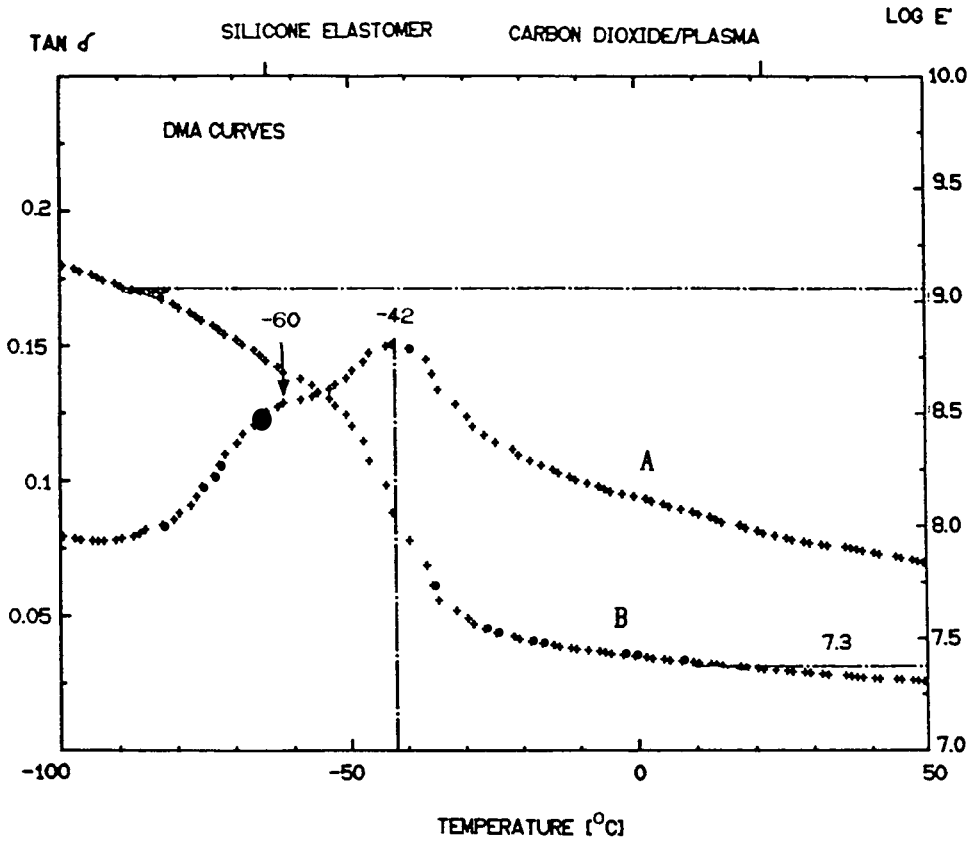


Fig. 10. DMA curves of CO₂/plasma surface modified elastomer: (A) tan δ; (B) log E'.

character of the network, as a result of the destructive nature of the gas/plasma treatment. Apparently, a destruction of some of the original junctions formed during the crosslinking process of the silicone network, followed by oxidation, lead to a greater flexibility of the polymer chains. However, in spite of the consistency of the $\log E'$ values, T_g 's do not follow this trend. Based on these results, it is clear that the T_g changes upon the treatment may or may not be related to the crosslink density, but represent contribution of the chemical structures that develop on the surface of the silicone network upon treatment. For example, one could visualize two networks where the segments between junction point have similar length, but the motion of the segments is different due the differences in chemical and structural composition of the segments. The latter will significantly effect T_g of each network.

As illustrated in Figure 10(A), in addition to the main T_g at -42.0°C , a shoulder at -60°C is observed. Similar to the argon-plasma treatment, this is attributed to the formation of oxidative products on the silicone rubber surface and is responsible for the secondary transitions. Such species as that illustrated in Figure 9 and deduced from the ATR FT-IR analysis lead to shorter segmental motions of chains at low temperatures.

Ammonia / Plasma Treatment

When gaseous ammonia is admitted to the plasma reaction chamber, drastic changes are observed in the surface ATR spectra. The plasma emission spectra of NH_3 have revealed the presence of NH_3 , NH_2 , NH , N_2 , H_2 , and H spectral features and various reactions have been postulated.^{34,35} Due to the presence of these highly reactive species, the $1800\text{--}1600\text{ cm}^{-1}$ region is dominated by the bands at 1664 and 1596 cm^{-1} . This is illustrated in Figure 11. In order to reveal the chemistry of the surface species generated upon such treatment, first it is necessary to understand the origin of the observed bands. While both bands are characteristic of the amide groups which are being formed during ammonia/plasma treatment, their precise assignment becomes essential. In general, the bands observed in this region indicate the presence of three types of amide groups: primary, monosubstituted, and disubstituted amides. Although one could observe that three types of amides can be present since the $\text{C}=\text{O}$ stretching vibration appears at 1664 cm^{-1} , the band at 1596 cm^{-1} indicates the formation of the NH groups. Thus, the assignment is narrowed down to the primary and monosubstituted amides. However, the monosubstituted amide NH bending normal vibrations would appear at 1550 cm^{-1} . Because this is not the case, the primary amides are a major component of the silicone rubber surface. This is schematically depicted in Figure 12. In order to confirm the above assignment, let us examine the NH stretching region of the spectra. This is shown in Figure 8(B), where two weak bands at 3350 and 3160 cm^{-1} due to symmetric and asymmetric NH stretching vibrations of the NH_2 groups are observed. Again, earlier attempts to detect such surface species upon the ammonia-plasma treatment resulted in failure.

Similar to the carbon dioxide-plasma treatment, let us examine ATR FT-IR spectra recorded with various angles of incidence. Figure 11 illustrates the changes in the relative band intensities of ammonia-plasma treated silicone

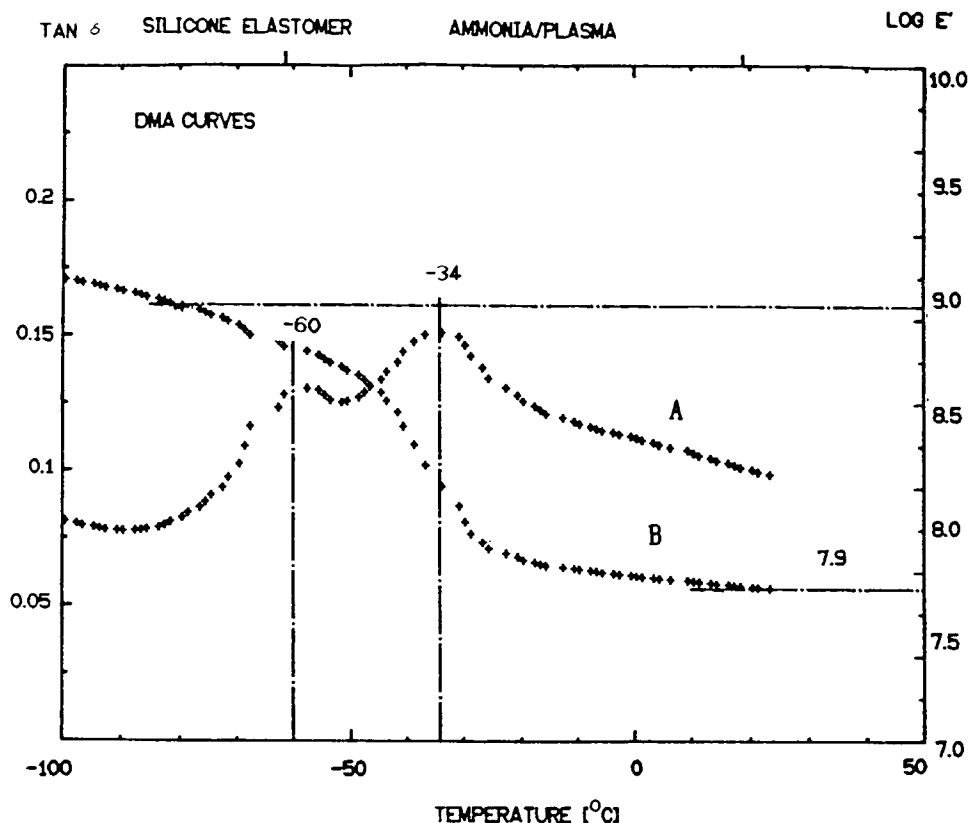


Fig. 13. DMA curves of ammonia/plasma treated silicone elastomer: (A) $\tan \delta$ curve; (B) $\log E'$ curve.

surface, as a function of incidence angle in ATR FT-IR measurements. Traces A and B show the spectra recorded with the 30° and 45° angles of incidence which correspond to approximately 5 and $3.3 \mu\text{m}$ depths of penetration at 1664 cm^{-1} , respectively. Trace B shows the increase of the band at 1664 cm^{-1} , indicating a greater amount of the amide groups present closer to the surface. Thus, the presence of the NH_2 functionalities on the silicone surfaces may be beneficial if one would like to graft other species onto the ammonia/plasma treated surfaces.

As discussed above, neither argon nor carbon dioxide plasma treatments result in an increase of crosslink density. On the other hand, plasma surface modification in the presence of ammonia leads to the increase of T_g to -34°C and $\log E'$ value to 7.9. This is illustrated in Figures 13(A) and (B), respectively. This observation by itself would indicate that, upon such treatment, the T_g increases due to the presence of primary amides on the surface of the silicone network and the increase of crosslink density. However, the ATR measurements clearly indicate that the amide groups are being formed, which have a naturally higher T_g than that of the silicone crosslinked network. At the same time, a new transition is observed at -60°C , which may be attributed to the presence of secondary transitions due to rotations of aliphatic carbonyl containing end-free segments of the surface. In light of the above

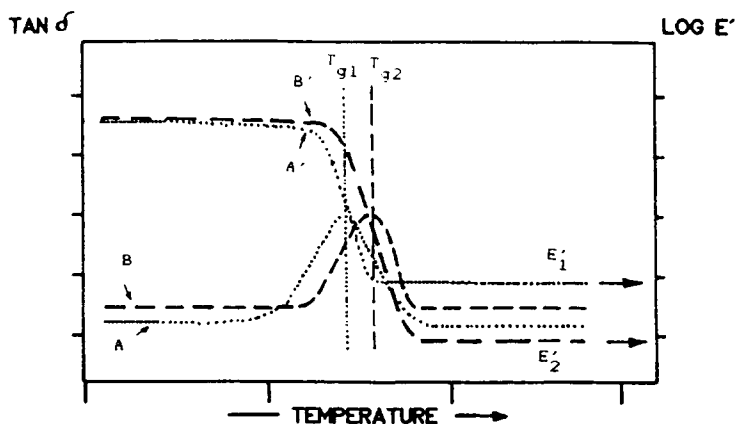


Fig. 14. An example of $\tan \delta$ and $\log E'$ curves with various degrees of crosslinking (see text for description).

considerations, it is appropriate to raise the question as to how amide groups themselves and hydrogen bonding influence the observed transitions. It is well established that the amide-containing polymers have a significantly higher thermal stability. In addition, a pronounced tendency of amide groups to form strong hydrogen bonding may greatly contribute to the improvement of mechanical integrity of the surface at elevated temperatures. As a result, higher T_g as well as the increased storage modulus are observed.

In summary, these studies indicate that, upon three different surface modifications of the silicone elastomer, T_g values cannot be used to even conceptually estimate the crosslink density. On the other hand, the storage modulus values provide an adequate means for such assessments. This is because a change in crosslink concentration may be accompanied by a change in chemical composition, which, in turn, may increase or decrease T_g , depending upon the chemistry involved. Apparently, these two factors should be included if one wants to estimate the crosslink density. To schematically depict a relationship between T_g and $\log E'$, Figure 14 was constructed. The first pair of curves, referred to as A and A', shows the reference T_g and $\log E'$ as a function of temperature. The second pair (B and B') indicates the increase of T_g and decrease of $\log E'$ values. This situation has already been shown for the silicone elastomer with the argon/plasma surface treatment and could hypothetically appear, if the sample was undercured and measurement temperatures did not exceed the curing temperature. In this case, the lower $\log E'$ values are indicative of less crosslinked network while T_g is related to the chemistry of a given system. Of course, one could also find that both $\log E'$ and T_g may increase as compared to the reference. Under such circumstances the elastomer would have been fully crosslinked (high $\log E'$) and T_g is greater since new chemical bonds have been formed upon curing.

CONCLUSIONS

In this work we have shown that by utilizing ATR FT-IR spectroscopy it is possible to monitor the formation of various surface structures developed upon plasma treatment in the presence of various gases. A combination of

spectroscopic measurements and dynamic mechanical analysis provides a suitable approach to establish that upon the plasma surface treatments, only ammonia/plasma leads to the increase of the $\log E'$ values, whereas argon and carbon dioxide treatments produce oxidative products which decrease the storage modulus above T_g . The enhancement of crosslink density is not observed. Although it is clear that in order to fully understand the effects of the silicone surface treatments, more work needs to be done. Our results indicate that what was believed in the past is not necessarily justified by suitable experiments. The surface crosslink density is not increased as a result of the highly energetic plasma environment but mostly produces new surface species on the silicone elastomer with shorter chains. Finally, we have shown that T_g values cannot be used as a means to estimate the crosslink density. A storage modulus is responsible for and should be used to analytically determine network properties.

The authors are grateful to Mr. Shubang Gan for providing help in the DMA measurements.

References

1. M. Gordon, T. C. Ward, and R. S. Whitney, *Polymer Networks*, A. J. Chompf and S. Newman, Eds., Plenum, New York, 1971.
2. L. C. DeBolt and J. E. Mark, *Macromolecules*, **20**, 2369 (1987).
3. D. R. Miller, E. M. Valles, and C. Macoscko, *Polym. Sci. Eng.*, **19**(4), 272 (1979).
4. Y. K. Leung and B. E. Eichinger, *J. Chem. Phys.*, **80**(8), 3877 (1984).
5. S. R. Gaboury and M. W. Urban, *Polym. Prepr.*, **30**(2), 356 (1988).
6. M. W. Urban and S. R. Gaboury, *Macromolecules*, **22**, 1486 (1989).
7. J. A. Hollahan and B. B. Stafford, *J. Appl. Polym. Sci.*, **13**, 807 (1969) and references therein.
8. N. Inagaki and K. Oh-Ishi, *J. Polym. Sci., Polym. Chem. Ed.*, **23**, 1445 (1985).
9. P. M. Triolo and J. D. Andrade, *J. Biomed. Mater. Res.*, **17**(1), 149 (1983).
10. N. J. DeLollis, *Natl. SAMPE Symp.*, **24**(2), 884 (1979).
11. S. L. DeGisi and C. H. Smith, in *SPE 36th Annu. Technol. Conf.*, SPE, Greenwich, CT, 1978, p. 675.
12. B. Arkles, *ChemTech*, **13**, 542 (1983).
13. N. J. DeLollis and Montoya, *J. Adhesion*, **3**, 57 (1971).
14. M. Suzuki, A. Kishida, H. Iwata, and Y. Ikada, *Macromolecules*, **19** 1804 (1986).
15. A. S. Chawla and R. Sipehia, *J. Biomed. Mater. Res.*, **18**, 537 (1984).
16. M. W. Urban and E. M. Salazar-Rojas, *Macromolecules*, **21**, 372 (1988).
17. N. Hasirci, *J. Appl. Polym. Sci.*, **34**(3), 1135 (1987) and references therein.
18. N. Inagaki and M. Taki, *J. Appl. Polym. Sci.*, **27**(11), 4337 (1982).
19. A. K. Hayes, *Thin Solid Films*, **84**(4), 401 (1981).
20. A. M. Wrobel, M. R. Wertheimer, J. Dib, and H. P. Schreiber, *J. Macromol. Sci. Chem.*, **A14**(3), 321 (1980).
21. T. Hirotsu, *J. Appl. Polym. Sci.*, **24**(9), 1957 (1979).
22. N. Inagaki, S. Kondo, and T. Murakami, *J. Appl. Polym. Sci.*, **29**(11), 3595 (1984).
23. G. Sachdev-Krishna and S. Sachdev-Harbans, *Thin Solid Films*, **107**(3), 245 (1983).
24. S. Chawla-Attar and R. Sipehia, *J. Biomed. Mater. Res.*, **18**(5), 537 (1984).
25. D. J. Cornelius and C. M. Monroe, *Polym. Eng. Sci.*, **25**(8), 467 (1985).
26. P. W. Rose and S. L. Kaplan, *Plasma Sci.*, **10**, 1 (1987).
27. C. Arnold, K. W. Bieg, R. E. Cuthrell, and G. C. Nelson, *J. Appl. Polym. Sci.*, **27**, 821 (1982).
28. L. W. Hill and K. Kozlowski, *J. Coat. Technol.*, **59**(751), 63 (1987).
29. S. Ikeda, *Prog. Org. Coatings*, **1**, 205 (1973).
30. J. Koralik, *Advances in Polymer Science*, Springer-Verlag, New York, 1982.
31. C. D. Armeniades, *J. Polym. Sci.*, **A-2**, **9**, 1345 (1971).

32. L. J. Bellamy, *The Infrared Spectra of Complex Molecules*, 3rd ed., Chapman and Hall, London, 1975.
33. N. B. Colthup, L. H. Daly, and S. E. Wiberley, *Introduction to Infrared and Raman Spectroscopy*, 2nd ed., Academic, New York, 1975.
34. G. L. Larson, D. Hernandez, I. Montes de Lopez Cepero, and L. E. Torres, *J. Org. Chem.*, **50**, 5260 (1985).
35. R. d'Agostino, F. Gramarossa, S. De Benedictis, and G. Ferraro, *Plasma Chem. Plasma Process.*, **1**, 19 (1981).

Received November 8, 1988

Accepted November 15, 1988